JOURNAL OF SOLID STATE CHEMISTRY **140,** 128–133 (1998)
ARTICLE NO. SC987874

A Monophosphate Molybdenum Bronze Built up from ReO_3-Type Slabs: $Ag_{0.7}Mo_3O_7(PO_4)$

S. Ledain, A. Leclaire, M. M. Borel, J. Provost, and B. Raveau

Laboratoire CRISMAT, UMR 6508 Associé au CNRS, ISMRA et Université de Caen, 6 Boulevard du Maréchal Juin, 14050 Caen Cedex, France

Received January 6, 1998; in revised form April 21, 1998; accepted April 30, 1998

A monophosphate molybdenum bronze $Ag_{2.8}(PO_2)_4(MoO_3)_{12}$ has been synthesized for the first time. This monoclinic bronze ($a = 23.857(3)$ Å, $b = 5.2990(6)$ Å, $c = 6.5659(4)$ Å, $\beta = 93.950(6)^\circ$), represents the $m = 6$ member of the $A_x(PO_2)_4(MO_3)_{2m}$ family (M = W, Mo). Its structure, which consists of ReO_3-type slabs interconnected with monophosphate groups, is very similar to those of the $m = 6$ members $K_x(PO_2)_4(WO_3)_{12}$ and Mo_4O_{11}, forming hexagonal tunnels where the Ag^+ cations are located. The distribtion of Ag^+ in the tunnels is however different from that of K^+ in the phosphate tungsten bronze: two sites are partially occupied close to the walls of the tunnels so that Ag^+ exhibits a ninefold and a tetrahedral coordination. The resistivity measurements, although performed on polyphasic samples, clearly show a semiconducting behavior. The possibility of charge density wave properties is considered. © 1998 Academic Press

INTRODUCTION

A tremendous amount of work has been devoted to the low-dimensional electronic properties of molybdenum bronzes these last twenty years. This is especially the case of several oxides such as Mo_4O_{11}, K_xMoO_3, or $K_xMo_6O_{17}$ which exhibit charge density wave (CDW) properties (for a review see Ref. (1)). In many of these bronzes, the presence of ReO_3-type slabs plays a crucial role for the appearance of CDW properties.

The discovery of phosphate tungsten bronzes, built up of ReO_3-type slices interconnected through phosphate groups (for reviews, see Refs. 2, 3), has opened a new direction for the exploration of low dimensional electronic systems. This is especially the case of monophosphate tungsten bronzes $(PO_2)_4(WO_3)_{2m}$, the CDW properties of which were evidenced six years ago (4–6) and are the object of intensive investigations to date (7, 8). The structural similarity between these phosphate tungsten bronzes and Mo_4O_{11} (9) is striking: the latter can be described as the member $m = 6$ of the series $(MoO_2)_4(MoO_3)_{2m}$ where MoO_4 tetrahedra and MoO_6 octahedra replace the PO_4 tetrahedra and WO_6 octahedra, respectively. This suggests the possibility to generate phosphate molybdenum bronzes with similar structures and CDW properties. In spite of this great analogy, all attempts to synthesize such phosphate molybdenum bronzes have been unsuccessful to date, leading to mixed valent molybdenum phosphates characterized by an electronic localization, with a different structure, where the Mo^{5+} and Mo^{6+} species are isolated (for a review see Ref. (3)). This different behavior of molybdenum can be explained by the peculiar electronic configuration of Mo(V) which tends to form a molybdenyl bond and consequently hinders any electronic delocalization.

The interpolation of a univalent cation into the Mo–P–O framework, such as Na^+, K^+, Rb^+, or Cs^+ is susceptible to change the Mo–O bonds, but unfortunately leads to different structures which imply also an electronic localization (3). We have thus tried to introduce Ag^+ species, which may influence differently the Mo–O bonds, owing to the more covalent character of silver compared to alkaline cations. In this paper, we report on the first monophosphate molybdenum bronze, $Ag_{2.8}(PO_2)_4(MoO_3)_{12}$, $m = 6$ member of the series $Ag_x(PO_2)_4(MoO_3)_{2m}$.

EXPERIMENTAL

Crystal Growth

Single crystals of this new compound were grown from a nominal composition $Li_{0.5}Ag_{0.5}Mo_2PO_8$. This compound has been synthesized in two steps: first $H(NH_4)_2PO_4$, MoO_3, Li_2CO_3, and $AgNO_3$ were mixed in an agate mortar in an adequate ratio and heated in air at 673 K in a platinum crucible to eliminate CO_2, NH_3, NO_2, and H_2O. In a second step the required amount of molybdenum was added and the resulting mixture was sealed in an evacuated silica ampoule then heated at 873 K for 24 h and cooled at 4.2 K per hour down to 773 K and finally quenched to room temperature.

Pink metallic platelike crystals were extracted from the so-obtained mixture. Their elementary analysis performed with an ISIS analyser mounted on scanning electron

0022-4596/98 $25.00

microscope Philips FEG XL30 allowed the cationic composition "$AgMo_3P$" composition to be established, in agreement with the formula deduced from the structure determination.

Different attempts to prepare a pure powder corresponding to the composition of the crystal, i.e. $Ag_{0.7}Mo_3PO_{11}$ were unsuccessful whatever the temperature. A polyphasic sample was systematically obtained where two major phases were present: $Ag_{0.7}Mo_3PO_{11}$ (about 70%) and the already known silver monophosphate $AgMo_3O_6(PO_4)_2$ (about 30%).

X-Ray Diffraction Study

Different crystals were tested by the Weissenberg method using Cu$K\alpha$ radiation.

A pink metallic crystal with dimensions $0.036 \times 0.136 \times 0.023$ mm^3 was selected for the structure determination. The cell parameters were determined by diffractometric techniques at 25°C with a least square refinement based upon 25 reflections with $18 < \theta < 22°$. The data were collected on a CAD4 Enraf-Nonius diffractometer with the parameters reported on Table 1. The systematic extinctions $h = 2n + 1$ for $h0l$ and $k = 2n + 1$ for $0k0$ are consistent with the space group $P2_1/a$. The reflections were corrected for the Lorentz and polarisation effects. The structure was solved with heavy atom method using the XTAL program.

TABLE 1
Summary of Crystal Data, Intensity Measurements, and Structure Refinement Parameters for $Ag_{2.8}(MoO_3)_{12}(PO_2)_4$

Crystal Data	
Space group	$P2_1/a$
Cell dimensions	$a = 23.857(3)$ Å
	$b = 5.2990(6)$ Å; $\beta = 93.950(6)°$
	$c = 6.5659(4)$ Å
Volume (Å)^3	828.1(1)
Z	8
ρ_{calc} (g cm^{-3})	4.57
Intensity Measurements	
λ(Mo$K\alpha$)	0.71073 Å
Scan mode	ω–θ
Scan width (deg)	$1.0 + 0.35 \tan\theta$
Slit aperture (mm)	$1.0 + \tan\theta$
Max θ (deg)	45
Standard reflections	3 measured every 3600 s
Measured reflections	7388
Reflections with $I > 3\sigma$	1811
Structure Solution and Refinement	
Parameters refined	90
Agreement factors	$R = 0.041$; $R_w = 0.051$
Weighting scheme	$w = 1/\sigma^2$
Δ/σ_{max}	<0.005

Transport Measurements

Resistivity measurements were performed on polyphasic sintered bars with nominal composition $Ag_{0.7}Mo_3PO_{11}$ with dimensions "$1.5 \times 1.5 \times 10$" mm^3, using the four-probe technique, in the temperature range 5–300 K.

RESULTS AND DISCUSSION

Structure

The refinement of the atomic coordinates and of the anisotropic thermal parameters for Mo and Ag, of the isotropic parameters for P and O, and of the occupancy factor for silver, allowed the reliability factors to be lowered to $R = 0.041$ and $R_w = 0.051$, for the atomic parameters listed in Table 2.

The projection of the structure of this new molydbenum monophosphate along $\vec{b}$ (Fig. 1) shows that it belongs to the family of monophosphate bronzes with hexagonal tunnels. Like the bronzes $Na_x(PO_2)_4(WO_3)_{2m}$ (11) and $K_x(PO_2)_4(WO_3)_8$ (12, 13), the structure of this new phase consists of ReO_3-type slabs connected through monophosphate groups, forming hexagonal tunnels along $\vec{b}$. The ReO_3-type slabs that form the host lattice consist of strings of six MoO_6 octahedra so that this new phase can be described as the member $m = 6$ of a possible monophosphate molybdenum bronze family with the generic formulation $Ag_x(PO_2)_4(MoO_3)_{2m}$. This result is of great interest, since

TABLE 2
Positional Parameters and Their Estimated Standard Deviations in $Ag_{2.8}(MoO_3)_{12}(PO_2)_4$

Atom	x	y	z	B (Å^2)	Occupation
Mo(1)	0.27871(5)	0.2383(4)	0.6707(2)	0.37(2)[a]	1
Mo(2)	0.40500(4)	0.2414(4)	0.3572(1)	0.34(4)[a]	1
Mo(3)	0.15665(4)	0.2319(4)	0.9966(2)	0.33(2)[a]	1
P(1)	0.0464(1)	0.2202(7)	0.3228(4)	0.20(4)	1
Ag(1)	0.5101(3)	0.2322(7)	0.8427(6)	1.15(6)[a]	0.55(2)
Ag(2)	0.4961(9)	0.211(2)	0.867(2)	1.15(6)[a]	0.14(2)
O(1)	0.2559(5)	0.530(2)	0.524(2)	0.7(2)	1
O(2)	0.3473(3)	0.226(2)	0.510(1)	0.6(2)	1
O(3)	0.3216(4)	0.445(2)	0.871(1)	0.6(2)	1
O(4)	0.3098(4)	0.942(2)	0.816(1)	0.6(2)	1
O(5)	0.0811(3)	0.256(3)	0.135(1)	0.90(8)	1
O(6)	0.4492(4)	0.450(2)	0.595(1)	0.8(2)	1
O(7)	0.4379(4)	−0.083(2)	0.513(1)	0.9(2)	1
O(8)	0.2155(3)	0.243(3)	0.829(1)	0.80(8)	1
O(9)	0.1103(4)	0.022(2)	0.778(1)	0.5(2)	1
O(10)	0.1209(4)	0.534(2)	0.842(1)	0.6(2)	1
O(11)	0.4855(3)	0.233(2)	0.239(1)	0.64(8)	1

[a] Atom anisotropically refined. Anisotropically refined atoms are given in the form of the isotropic equivalent displacement parameter defined as $B = \frac{4}{3}\sum_i\sum_j \vec{a}_i\vec{b}_j\beta_{ij}$.

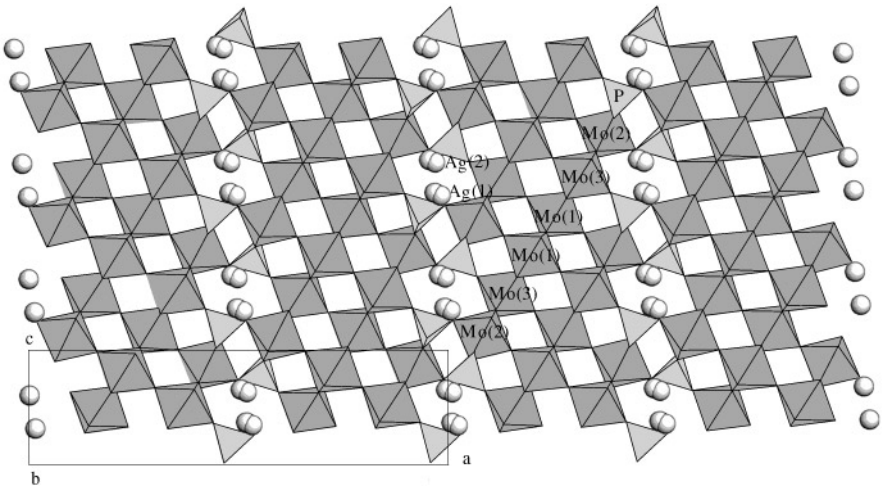

FIG. 1. Projection of the $Ag_{2.8}(PO_2)_4(MoO_3)_{12}$ structure along $\vec{b}$.

such a framework has never been observed before in molybdenum phosphates. Thus $Ag_{2.8}(PO_2)_4(MoO_3)_{12}$ is the unique molybdenum phosphate bronze that has been synthesized to date. Moreover, this bronze can be compared to the tungsten phosphate bronze $Na_x(PO_2)_4(WO_3)_{12}$ (11) and to the monoclinic oxide Mo_4O_{11}, i.e. $(MoO_2)_4(MoO_3)_{12}$ (9) which are both $m = 6$ members, with PO_4 or MoO_4 tetrahedra ensuring the connection between octahedral "WO_3" or "MoO_3" layers, respectively.

The interatomic distances (Table 3) show that the MoO_6 octahedra are strongly distorted, as for $Na_x(PO_2)_4(WO_3)_{12}$ and for the monoclinic form of Mo_4O_{11}. Like these two bronzes, the monophosphate molybdenum bronze exhibits two sets of Mo–O distances: three long Mo–O bonds and three shorter ones.

The distortion of the MoO_6 octahedra increases with the number of Mo–O–P bonds. The Mo(1) octahedron which is linked to six MoO_6 octahedra is indeed the less distorted with two sets of Mo–O distances ranging from 1.84 to 1.89 Å and from 1.949 to 2.008 Å, respectively. In contrast the Mo(2) octahedron which shares its apices with three MoO_6 octahedra and three PO_4 tetrahedra is the most distorted with two sets of Mo–O distances ranging from 1.757 to 1.789 Å and from 2.12 to 2.13 Å, respectively. The Mo(3) octahedron which is linked to five MoO_6 octahedra and one PO_4 tetrahedron adopts an intermediate configuration with two sets of Mo–O distances, ranging from 2.047 to 2.078 Å and from 1.807 to 1.844 Å, respectively. Note that the Mo–O distances which correspond to the Mo–O–P bonds are the longest due to the more covalent character of phosphorus. Such an evolution is also observed for Mo_4O_{11} and for $Na_x(PO_2)_4(WO_3)_{12}$, so that the sets of distances observed for these two structures are very similar to those obtained for $Ag_{2.8}(PO_2)_4(MoO_3)_{12}$. In all these structures the PO_4 tetrahedra remain practically regular, as shown here for the P–O bonds which range from 1.53 to 1.54 Å. Finally it is worth pointing out that the MoO_6 octahedra of two successive strings are tilted with respect to each other, compensating the distortion of the octahedra.

The Ag^+ cations are located, like the Na^+ cations of $Na_x(PO_2)_4(WO_3)_{12}$, in the hexagonal tunnels of the structure. However, there are several remarkable differences between the two compounds. The first one concerns the silver content—2.8 Ag^+ per $(PO_2)_4$ formula—which is much higher than that observed for all the sodium phosphate bronzes (1.5–1.7 Na^+ per $(PO_2)_4$ formula). The second difference deals with the location of silver in the tunnels and consequently its coordination compared to sodium. In the sodium bronze the Na^+ cation is located in one site close to the wall of the tunnels: it exhibits four closest oxygen neighbors with Na–O distances ranging from 2.45 to 2.64 Å, and five other oxygen atoms are located significantly further apart (2.91–3.12 Å). In the silver phosphate bronze, Ag^+ is also located near the walls of the tunnels but it is distributed over two sites which can be described as a splitting of the Na^+ site, so that they cannot be occupied simultaneously (Fig. 1). The Ag(1) site, with an occupancy factor of 0.55, exhibits a ninefold coordination with Ag(1)–O distances regularly distributed from 2.40 to 3.15 Å (Table 3). The $Ag(1)O_9$ polyhedron very different from that of sodium can then be described as a distorted monocapped hexagonal bipyramid. In the Ag(2) site, with an occupancy factor of 0.14, silver exhibits a rather regular tetrahedral coordination with four Ag–O distances ranging from 2.40 to 2.60 Å; five other oxygen atoms are located much further apart at distances ranging from 3.03 to 3.16 Å. It is likely that the strong tendency of silver to form covalent bonds in this structure favors its stability.

TABLE 3
Distances (Å) and Angles (deg) in the Polyhedra in $Ag_{2.8}(MoO_3)_{12}(PO_2)_4$[a,b]

Mo(1)	O(2)	O(1)	O(8)	O(3)	O(4)	O(1)[i]
O(2)	**2.008(8)**	2.67(1)	3.90(1)	2.75(1)	2.71(1)	2.72(1)
O(1)	87.6(4)	**1.84(1)**	2.71(1)	3.79(1)	2.68(1)	2.68(1)
O(8)	178.0(4)	93.0(5)	**1.899(8)**	2.75(1)	2.76(1)	2.74(1)
O(3)	88.0(4)	174.9(5)	91.4(4)	**1.949(9)**	2.70(1)	2.72(1)
O(4)	86.2(4)	89.7(4)	91.9(5)	87.5(4)	**1.96(1)**	3.83(1)
O(1)[i]	88.6(5)	92.1(5)	93.3(5)	90.3(4)	174.5(4)	**1.88(1)**

Mo(2)	O(2)	O(11)	O(9)	O(6)	O(10)	O(7)
O(2)	**1.760(8)**	3.85(1)	2.71(1)	2.73(1)	2.68(1)	2.71(1)
O(11)	166.2(3)	**2.122(8)**	2.75(1)	2.80(1)	2.77(1)	2.76(1)
O(3)	100.6(5)	89.7(4)	**1.757(9)**	2.77(1)	2.63(1)	3.87(1)
O(6)	88.5(4)	82.2(4)	98.4(4)	**2.133(9)**	3.91(1)	2.88(1)
O(10)	98.3(4)	89.6(4)	95.8(4)	169.8(4)	**1.789(9)**	2.71(1)
O(7)	88.1(5)	81.0(4)	170.2(4)	85.4(4)	87.3(4)	**2.12(1)**

Mo(3)	O(8)	O(4)	O(9)	O(3)	O(5)	O(10)
O(8)	**1.844(8)**	2.67(1)	2.77(1)	2.72(1)	3.90(1)	2.74(1)
O(4)	94.0(4)	**1.807(9)**	3.87(1)	2.67(1)	2.78(1)	2.74(1)
O(9)	89.7(4)	173.1(4)	**2.074(9)**	2.75(1)	2.79(1)	2.75(1)
O(3)	96.2(5)	95.4(4)	90.1(4)	**1.81(1)**	2.85(1)	3.85(1)
O(5)	168.1(4)	91.1(4)	84.3(4)	94.1(5)	**2.078(8)**	2.65(1)
O(10)	89.3(5)	90.3(4)	83.9(4)	171.8(4)	79.9(4)	**2.047(9)**

P	O(11)	O(6)	O(7)	O(5)
O(11)	**1.539(8)**	2.49(1)	2.49(1)	2.43(1)
O(6)	108.5(6)	**1.53(1)**	2.55(1)	2.54(1)
O(7)	108.7(6)	112.5(5)	**1.53(1)**	2.53(1)
O(5)	103.9(4)	111.7(7)	111.1(6)	**1.542(9)**

Ag(1)–O(6)	2.40(1) Å	Ag(2)–O(11)[iii]	2.50(2) Å
Ag(1)–O(11)[vi]	2.705(9) Å	Ag(2)–O(5)[ii]	2.60(2) Å
Ag(1)–O(9)[iv]	2.78(1) Å	Ag(2)–O(11)[vi]	2.47(2) Å
Ag(1)–O(5)[ii]	2.474(9) Å	Ag(2)–O(9)[iv]	3.16(2) Å
Ag(1)–O(7)[iii]	2.83(1) Å	Ag(2)–O(6)	2.40(2) Å
Ag(1)–O(11)[v]	2.89(1) Å	Ag(2)–O(5)[vii]	3.03(2) Å
Ag(1)–O(11)[iii]	2.52(1) Å	Ag(2)–O(7)[iii]	3.11(2) Å
Ag(1)–O(10)[iv]	3.00(1) Å	Ag(2)–O(7)	3.05(2) Å
Ag(1)–O(7)[i]	3.15(1) Å	Ag(2)–O(11)[v]	3.07(2) Å

[a]The Mo–O or P–O distances are on the diagonal, above it are the O ⋯ O distances, and below are the O–Mo–O or O–P–O angles.

[b]Symmetry codes: i, $1/2 - x$, $1/2 + y$, $-z$; ii, $x + 1/2$, $y - 1/2$, z; iii, $x - 1$, y, $z - 1$; iv, $x - 1/2$, $y - 1/2$, z; v, $x - 1$, $y - 1$, $z - 1$; vi, x, y, $z + 1$; vii, $x - 1/2$, $y + 1/2$, $z - 1$.

Electronic Delocalization

The absence of a configuration characteristic of the molybdenyl ion, contrary to what is often observed for Mo(V) in molybdenum phosphates, suggests a possible delocalization of the electrons in the $[MoO_3]_\infty$ slabs. The electrostatic valence distribution calculated with the Brese and O'Keeffe (10) expression, with $R_{ij} = 1.879$ supports this viewpoint. Valencies of 5.42, 5.59, and 5.33 are obtained for Mo(1), Mo(2), and Mo(3), respectively. These values are in agreement with the average oxidation state of molybdenum of 5.43 deduced from the chemical formula. Note also that these calculations are in agreement with the valencies of P, Ag, and O species in such oxides (Table 4). It is worth pointing out that Mo(1) which is only linked to MoO_6 octahedra exhibits a valence of 5.42 close to the value corresponding to the perfect electronic delocalization (5.43), whereas on the opposite Mo(2) which is linked to three PO_4 tetrahedra tends to increase its oxidation state (5.59).

Although they cannot be considered as accurate, the resistivity measurements performed on sintered bars of polyphasic samples are of great interest. Indeed, as the minor phase $AgMo_3O_6(PO_4)_2$ is built on trioctahedral Mo_3O_{13} isolated units and is an insulator, the thermal behavior of the electrical resistance of the sintered bar can be ascribed to the behavior of the major phase. The data

TABLE 4
Electrostatic Valence Distribution for $Ag_{2.8}(MoO_3)_{12}(PO_2)_4$[a]

	Mo(1)	Mo(2)	Mo(3)	P(1)	Ag(1)	Ag(2)	$\sum v_i^-$
O(1)	1.111						2.11
	0.997						
O(2)	0.706	1.379					2.09
O(3)	0.828		1.205				2.03
O(4)	0.803		1.215				2.02
O(5)			0.584	1.182	0.075	0.101	
						0.031	
					0.091	0.016	1.88
						0.005	
O(6)		0.503		1.221	0.090	0.172	
					0.110	0.028	1.86
O(7)		0.521		1.221	0.028	0.025	
					0.012	0.030	
					0.035	0.004	1.80
					0.014	0.005	
O(8)	0.973		1.099				2.07
O(9)		1.391	0.590		0.0324	0.022	
					0.0396	0.004	2.02
O(10)		1.275	0.635		0.018		
					0.021		1.93
O(11)		0.519		1.192	0.040	0.132	
					0.024	0.143	
					0.065	0.033	
					0.048	0.021	1.91
					0.029	0.023	
					0.080		
$\sum v_i^+$	5.42	5.59	5.33	4.82	0.85	0.80	

[a]In the Ag column, due to the partial occupation of the three sites, for each oxygen atom the first line corresponds to the electrostatic valencies received by the oxygen atoms from the cations taking into account the silver population; the sum of the two lines corresponds to the electrostatic valencies received by the cations from the oxygen atoms.

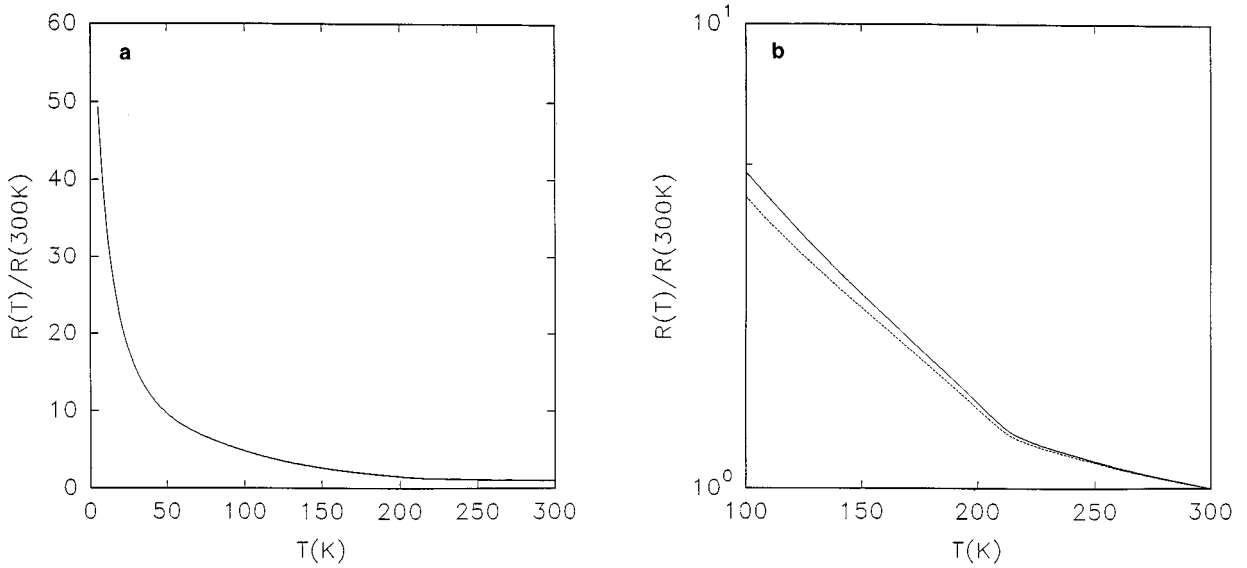

FIG. 2. (a) The typical resistance ratio $R(T)/R(300\text{ K})$ versus T for a polyphasic sintered bar shows the semiconducting behavior of the conductivity. (b) Logarithmic plot of $R(T)/R(300\text{ K})$ for two sintered samples. This plot shows the change in the shape at $T = 215\text{ K}$.

were not analyzed in terms of resistivity due to the polyphasic character of the bars but only in terms of resistance normalized to the value at 300 K: $R(T)/R(300\text{ K})$. The normalized resistance $R(T)/R(300\text{ K})$ of a sintered bar has been plotted on Fig. 2a which shows the semiconducting behavior of the conductivity. The resistance $R(300\text{ K})$ is rather low ($\sim 1\ \Omega$) and is multiplied by a factor of 50 between 300 and 5 K. On Fig. 2b the ratio $R(T)/R(300\text{ K})$ has been plotted in a logarithmic scale in the temperature range $100 < T < 300\text{ K}$ for two sintered bars. For the two bars, the latter curve shows a significant variation of the resistance at $T = 215\text{ K}$. It is worth comparing the electron transport properties of this monophosphate molybdenum bronze $Ag_{2.8}(PO_2)_4(MoO_3)_{12}$ with those of other two-dimensional conductors, such as $La_2Mo_2O_7$ (14–17) and $K_x(PO_2)_4(WO_3)_8$ (18).

The first time, $La_2Mo_2O_7$ exhibits a different behavior according to the others, i.e., metallic along $\vec{c}$ according to Ref. (15), sample-dependent according to Ref. (16), and semiconducting according to Ref. (17). Semi-conducting behavior is shown in Ref. (16), with the current parallel to the $\vec{b}$ axis, i.e., perpendicular to the (010) Mo_2O_7 layers of corner-sharing MoO_6 octahedra. It is remarkable that in the three references (15–17) a phase transition occurs at $T \approx 125\text{ K}$ which is ascribed to a CDW transition, confirmed by magnetic susceptibility measurements (15, 16).

In the monophosphate tungsten bronze $K_x(PO_2)_4(WO_3)_8$, a CDW transition has been recently discovered (18). The structure of $Ag_{2.8}(PO_2)_4(MoO_3)_{12}$ is closely related to that of $K_x(PO_2)_4(WO_3)_8$ which is the $m = 4$ member of the series.

The variation of resistance at $T = 215\text{ K}$ observed for our sample should be related to a CDW transition which is known to occur in low-dimensional compound and particularly in the two compounds considered above showing a related structure.

It must be borne in mind that the electrical resistance has been measured on a ceramic sample, and consequently the measured resistance is an effective value mixing the resistivity along the $\vec{a}$, $\vec{b}$, and $\vec{c}$ axes of the crystallites. The transport properties should be metallic in the ReO_3-type slabs and semi-conducting when the current flows perpendicular to the slabs.

Attempts are in process to grow single crystals, in order to confirm or invalidate the metallic character of the conductivity in the ReO_3-type slabs. Other physical studies such as the thermopower and the magnetic susceptibility measurements should provide more information about CDW transition.

REFERENCES

1. "Low-Dimensional Electronic Properties of Molybdenum Bronzes and Oxides" (C. Schlenker, Ed.), Physics and Chemistry of Materials with Low-Dimensional Structures Series, Vol. 11. Kluwer Acad. Publ. Dordrecht, The Netherlands, 1989.
2. B. Raveau, *Proc. Indian Acad. Sci.* **96,** 419 (1986).
3. M. M. Borel, M. Goreaud, A. Grandin, Ph. Labbé, A. Leclaire, and B. Raveau, *Eur. J. Solid State Inorg. Chem.* **28,** 93–129 (1991).
4. M. H. Whangbo, E. Canadell, P. Foury, and J. P. Pouget, *Science* **252,** 96 (1991).
5. E. Wang, I. E. Rachidi, E. Canadell, M. H. Whangbo, and S. Vadlamannati, *Phys. Rev. B* **39,** 12969 (1989).

6. Z. S. Teweldemedhin, K. V. Ramanujachari, and M. Greenblatt, *Phys. Rev. B* **46,** 7897 (1992).
7. C. Schlenker, C. Hess, C. Le Touze, and J. Dumas, *J. Phys. I France* **6,** 2061 (1996).
8. A. Ottolenghi and J. P. Pouget, *J. Phys. I France* **6,** 1059 (1996).
9. L. Kihlborg, *Arkiv Kemi* **21,** 365 (1963).
10. N. E. Brese and M. O'Keeffe, *Acta Crystallogr. Sect. B* **47,** 192 (1991).
11. A. Benmoussa, D. Groult, Ph. Labbé, and B. Raveau, *Acta Crystallogr. Sect. C* **40,** 573 (1984).
12. J. P. Giroult, M. Goreaud, Ph. Labbé, and B. Raveau, *J. Solid State Chem.* **44,** 407 (1982).
13. B. Domengès, M. Hervieu, B. Raveau, and M. O'Keefe, *J. Solid State Chem.* **72,** 155 (1988).
14. W. H. McCaroll, C. Darling, and G. Jakubicki, *J. Solid State Chem.* **48,** 189 (1983).
15. A. Moini, M. A. Subramanian, A. Clearfield, F. S. Di Salvo, and W. H. McCaroll, *J. Solid State Chem.* **66,** 136 (1987).
16. B. T. Collins, M. Greenblatt, W. H. McCaroll, and G. W. Hull, *J. Solid State Chem.* **73,** 507 (1988).
17. K. Surendramath, C. Bansal, M. Greenblatt, and W. H. McCaroll, *Phys. Rev. B* **40**, 9312 (1989).
18. P. Roussel, D. Groult, C. Hess, Ph. Labbé, and C. Schlenker, *J. Phys. Condens. Matter* **9,** 7081 (1997).